A slip model for the spherical actuation of the Atlas motion platform

Article *in* Transactions- Canadian Society for Mechanical Engineering · December 2005

DOI: 10.1139/tcsme-2005-0048

3 authors, including:

M. J. D. Hayes
Carleton University
86 PUBLICATIONS **556** CITATIONS

SEE PROFILE

A SLIP MODEL FOR THE SPHERICAL ACTUATION OF THE ATLAS MOTION PLATFORM

J.B. Holland, M.J.D. Hayes and R.G. Langlois
Department of Mechanical andAerospace Engineering, Carleton University,
Ottawa, Ontario, Canada
Contact: jhayes@mae.carleton.ca

Received July, 2005, Accepted December, 2006
No. R05-CSME-44, E.I.C. Accession 2896

Abstract

The Atlas platform represents a novel six degree-of-freedom motion platform architecture. Orienting is decoupled from positioning, and unlimited rotations are possible about every axis. The decoupling is accomplished by fixing a three degree-of-freedom spherical orienting device, called the Atlas sphere, on a gantry with three orthogonal linear axes. The key to the design is three omni-directional wheels in an equilateral arrangement, which impart angular displacement to a sphere, providing rotational actuation. The free-spinning castor rollers provide virtually friction-free motion parallel to each omni-wheel rotation axis creating the potential for unconstrained angular motion. Since the sphere directly contacts the omni-wheels, there are no joints or links interfering with its motion, allowing full 360º motion about all axes. However, the kinematic constraints are non-holonomic. This paper explores the slip at the interface between each omni-wheel and the Atlas sphere. A kinematic slip model is presented, introducing the *slip ratio*, which is the ratio of the k^{th} omni-wheel's transverse velocity component, $\mathbf{S}_{\perp_k}$, which is perpendicular to the free-spinning castor wheel axis, and the tangential velocity component, $\mathbf{S}_{tank}$, which is perpendicular to the omni-wheel driving axis, parallel to the tangential velocity vector, $\mathbf{V}_k$. The long-term goal is to incorporate the slip model into a control law for position level control of the sphere. Two illustrative examples are given.

UN MODÈLE DE GLISSADE POUR LA MISE EN ACTION SPHÉRIQUE DE LA PLATEFORME DE MOUVEMENT D'ATLAS

Résumé

La plateforme d'Atlas représente une architecture de plateforme de mouvement de degré-de-liberté du roman six. Orientant est découplé du positionnement, et les rotations illimitées sont possibles autour de chaque axe. Le découplage est accompli en fixant un dispositif d'orientation sphérique de la degré-de-liberté trois, appelé la sphère d'Atlas, sur un portique avec trois haches linéaires orthogonales. La clef à la conception est trois omnidirectionnels roule dedans un arrangement équilateral, qui donnent l'écart angulaire à une sphère, fournissant la mise en action de rotation. Les rouleaux derotation de roulette fournissent le mouvement pratiquement frottement-libre paralléle à chaque axe de rotation d'omni-roue créant le potentiel pour le mouvement angulaire sans contrainte. Puisque la sphère entre en contact avec directement les omni-roues, il n'y a aucun joint ou lien interférant son mouvement, permettant le plein mouvement 360º autour de toutes les haches. Cependant, les contraintes cinématiques sont non-holonomic. Cet article explore la glissade à l'interface entre chaque omni-roue et la sphère d'Atlas. Un modèle cinématique de glissade est présenté, présentation rapport de glissade de (rapport de chaque vitesse tangentielle d'omni-roue à l'interface à cela de la sphère au même point). Le but à long terme est d'incorporer le modèle de glissade à une loi de commande pour la commande de niveau de position de la sphère. Deux exemples d'illustration sont donnés.

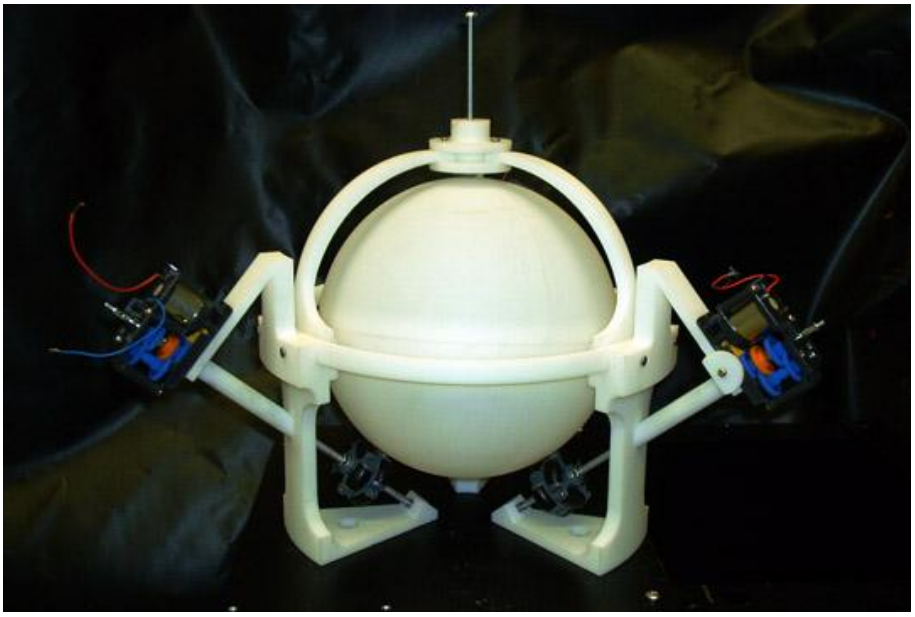

Figure 1: Atlas proof-of-concept demonstrator.

1 Introduction

The Atlas platform, pictured in Figure 1, is a novel conceptual design resulting from the Carleton University Simulator Project (CUSP), see [1, 2]. The Atlas sphere is driven by the three omni-wheels [3, 4], which allows unlimited angular displacement about any (every) axis through the geometric centre of the sphere. The angular velocity of the sphere is proportional to a linear combination of the angular velocities, less the free spinning across the castors on the periphery of each omni-wheel, less the slip and scrub on the castors. In most cases the sphere's tangential velocity at the contact point of each omni-wheel and that of the corresponding point on the omni-wheel itself will be different. This will produce slip at the three contact points as well as scrub.

For clarity in the context of this paper, *slip* refers to differences in translational velocity whereas *scrub* refers to differences in angular velocity between contacting bodies. The focus of this paper is limited to slip. Spherical platform velocity-level kinematics and the associated Jacobian matrix relating omni-wheel angular velocities to the angular velocity of the Atlas sphere, developed in [2], are used to investigate the slip behaviour of the Atlas sphere on the three driving omni-wheels.

The concept of a spherical actuator is not new. Spherical DC induction motors were introduced in 1959 by Williams, et al. in [5]. Developments continued over the next 30 years leading to designs presented in [6, 7, 8], for example. However, due to physical limitations imposed by the stator and commutator angular displacements are limited.

2 Atlas Platform Description

Detailed descriptions of the Atlas platform evolution and kinematic geometry can be found in [1, 2]. The Atlas sphere is driven by three omni-wheels. This in turn is an adaptation of three-omni-wheeled vehicles that move in the plane [9]. Friction between the omni-wheels and sphere is

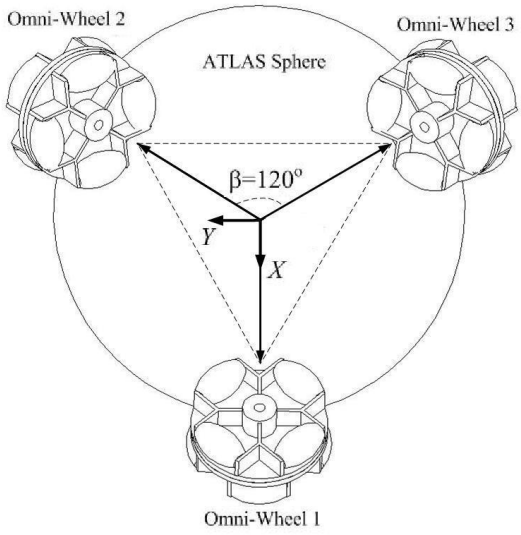

Figure 2: Omni-wheel axes projected in the XY-plane shown from the bottom view.

maintained by gravity (the weight of the sphere lies evenly on the three omni-wheels), and by a downward force applied at the north pole of the sphere by a spring loaded ball bearing mounted to the frame (this system can be seen in Figure 1).

Because the castors are free-spinning, they allow the sphere to spin in directions perpendicular to the rotation axes of the castor wheels. The omni-wheels thereby enable an unlimited rotational capability for the Atlas sphere allowing for 360° displacements in roll (about the X-axis), pitch (about the Y-axis), and yaw (about the Z-axis), as well as any linear combination. The right-handed $[X, Y, Z]$ coordinate system is identified in Figure 2.

For the kinematic analysis of the Atlas platform [2] seven reference coordinate frames were needed. The first being the inertial frame $[X, Y, Z]$ which is centred in the middle of the omni-wheel triangle, illustrated in Figure 2. The inertial frame ($[X, Y, Z]$) has its X-axis pointing to Omni-wheel 1, and its Z-axis perpendicular to the contact point plane which will be denoted the XY-plane.

The origins of the next three reference frames are on the centre of each omni-wheel. The x-axis

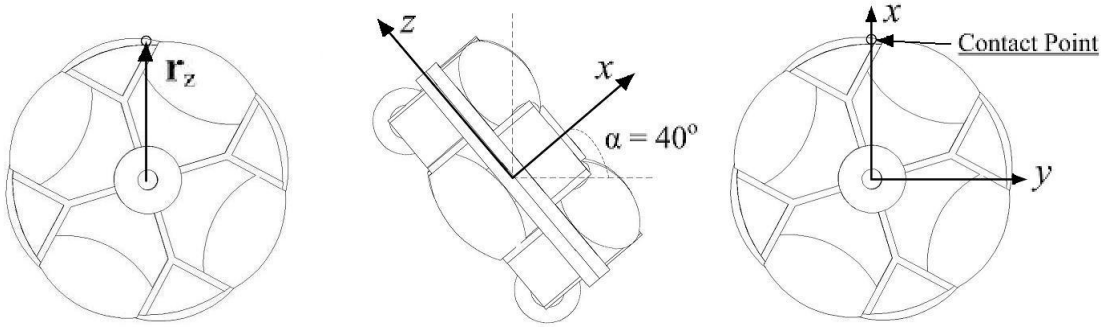

Figure 3: Omni-wheel coordinate reference frames.

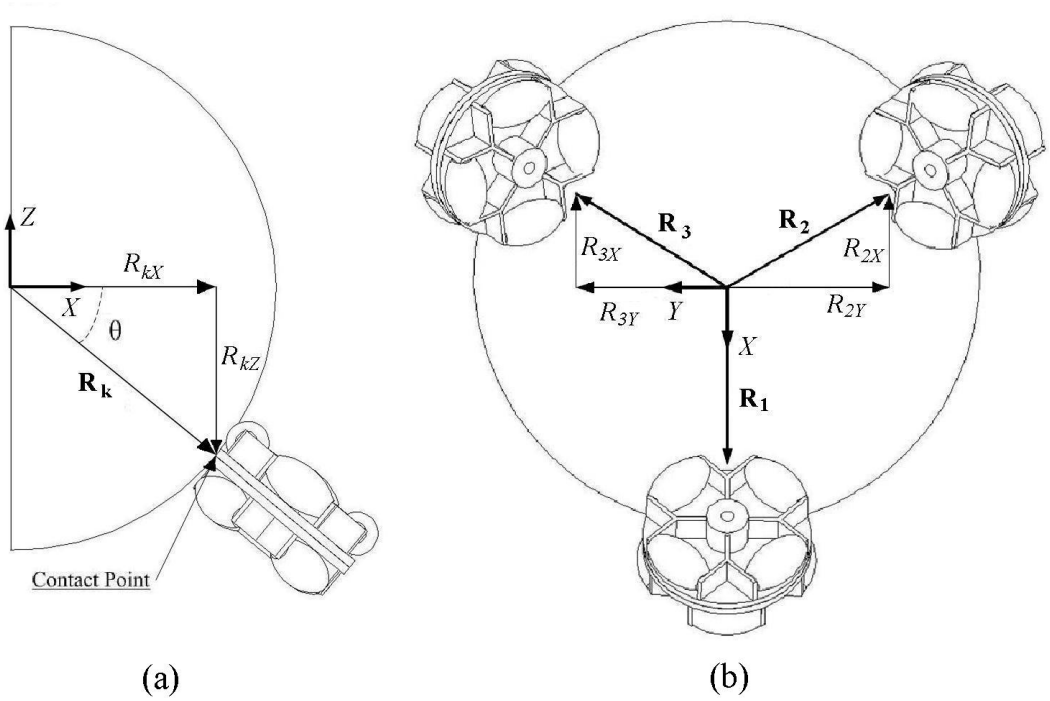

Figure 4: Sphere contact point radial vector components: (a) side view; (b) bottom view.

points outwards from the wheel centre and the z-axis points towards the contact point between the omni-wheel and Atlas sphere, illustrated in Figure 3. Each omni-wheel frame will be designated $[x_k,y_k,z_k]$ where $k \in \{1,2,3\}$, indicating each omni-wheel; for instance, the frame of omni-wheel two will be designated $[x_2,y_2,z_2]$. The linear velocity at the contact point expressed in the k^{th} omni-wheel frame is computed as the cross product of the omni-wheel angular velocity vector, $\boldsymbol{\omega}_k$, and the radial vector pointing from the omni-wheel centre to the contact point in the z-direction, $\mathbf{r}_k$. The remaining three reference frames originate, one each, at each omni-wheel contact point with the sphere, but are not rotated by the tilt of the omni-wheel; this will allow for easier analysis when studying the slip factors existing at the contact points. These frames are the omni-wheel slip frames and designated $[i_k,j_k,k_k]$, again where k indicates the wheel being considered.

The actual dimensions of the omni-wheel angular separation are dependent on the diameter of the Atlas sphere and how high the centre of the sphere will be relative to the XY-plane. The centre of the sphere can be located anywhere relative to the XY-plane. The optimal location of the Atlas sphere's centre will not be discussed in this paper and will be left as a variable. The radius vector of the Atlas sphere is the position vector of each omni-wheel contact point, expressed in $[X,Y,Z]$ as $\mathbf{R}_k$, having components $[R_{k_X}, R_{k_Y}, R_{k_Z}]$, with k indicating a particular omni-wheel, see Figure 4. Since the omni-wheel contact points are the vertices of an equilateral triangle, the norm of each radius vector is the same:

$$\|\mathbf{R}_1\| = \|\mathbf{R}_2\| = \|\mathbf{R}_3\| = \|\mathbf{R}\|. \tag{1}$$

The angle θ varies with the ratio of R_{k_Z} and R_{k_X}:

$$\theta \;=\; \text{atan2}\left(\frac{R_{k_Z}}{R_{k_X}}\right). \tag{2}$$

Since $\mathbf{R}_1$ is situated along the X-axis there is no R_{1_Y} component, only R_{1_X} and R_{1_Z}. The $\mathbf{R}_1$ vector points from the centre of the Atlas sphere towards the contact point of Omni-wheel 1 so R_{1_X} is always positive while R_{1_Z} is always negative. As stated earlier, R_{1_X} and R_{1_Z} are left as variables for the user to define, as the optimal locations for the contact points relative to the sphere is not an issue addressed in this paper. To determine the radial vectors $\mathbf{R}_2$ and $\mathbf{R}_3$, vector $\mathbf{R}_1$ can be transformed using rotation matrices defined by the geometry of the Atlas sphere configuration illustrated in Figure 4. These transformations were also used in determining the orienting Jacobian and for characterizing sphere slip on the omni-wheels of the Atlas platform.

Two angles must be considered when calculating these transformations, α and β. The angle α, see Figure 3, is the tilt of the omni-wheel about the omni-wheel y-axis. For the current configuration, $\alpha = 40^\circ$ for each wheel, with counter-clockwise rotations being positive. The angle β, see Figure 2, represents the rotation of each omni-wheel axis about the Z-axis, relative to the axis of Omni-wheel 1. Thus $\beta_1 = 0^\circ$, $\beta_2 = 120^\circ$, and $\beta_3 = 240^\circ$.

3 Relevant Kinematics

Velocity-level kinematics corresponding to the Atlas motion system, as developed by Robinson et al [2], required for developing the slip model are reproduced here. Readers are referred to the original paper for the complete derivation. The Atlas sphere kinematics were developed based on two angular velocity vectors: the angular velocity of the sphere expressed in the global-frame $[X, Y, Z]$ is denoted $\mathbf{\Omega}$, while the collection of three omni-wheel angular velocities about their shaft axes expressed in the omni-wheel coordinate frames $[x_k, y_k, z_k]$ is denoted $\boldsymbol{\omega}_k$, $k \in \{1, 2, 3\}$.

The tangential velocities at the respective sphere contact points lie along the k^{th} omni-wheel local y-axes and are denoted

$$\mathbf{v}_k \;=\; [0, v_{k_y}, 0]^T \;=\; \boldsymbol{\omega}_k \times \mathbf{r}_k, \tag{3}$$

where $\boldsymbol{\omega}_k$ and $\mathbf{r}_k$ are the k^{th} omni-wheel angular velocity and radial vectors (directed from the omni-wheel centre to the sphere contact point, see Figure 3). These velocity vectors are mapped from their respective omni-wheel coordinate frames $[x_k, y_k, z_k]$ to the global frame $[X, Y, Z]$ using geometric transformations having the form:

$$\mathbf{T}_k \;=\; \begin{bmatrix} \mathrm{c}_{\beta_k} & \mathrm{s}_{\beta_k} & 0 \\ -\mathrm{s}_{\beta_k} & \mathrm{c}_{\beta_k} & 0 \\ 0 & 0 & 1 \end{bmatrix}, \tag{4}$$

where c_{β_k}, and s_{β_k} respectively denote $\cos\beta_k$ and $\sin\beta_k$; it is possible to express the tangential velocities $\mathbf{V}_k$ at the contact points in the inertial frame:

$$\mathbf{V}_1 \;=\; [0 \;\; -\omega_1 r_z \;\; 0]^T, \tag{5}$$

$$\mathbf{V}_2 \;=\; [-\omega_2 r_z \mathrm{s}_{\beta_2} \;\; -\omega_2 r_z \mathrm{c}_{\beta_2} \;\; 0]^T, \tag{6}$$

$$\mathbf{V}_3 \;=\; [-\omega_3 r_z \mathrm{s}_{\beta_3} \;\; -\omega_3 r_z \mathrm{c}_{\beta_3} \;\; 0]^T. \tag{7}$$

Further derivation results in the relationship between omni-wheel angular velocities, $\boldsymbol{\omega}$, and the sphere angular velocity, $\boldsymbol{\Omega}$, that reveals the system Jacobian matrix $\mathbf{J}$, which is independent of any time varying parameters and is therefore constant [2]:

$$\boldsymbol{\Omega} \;=\; \mathbf{J}\boldsymbol{\omega} \;=\; \frac{r_z}{\|\mathbf{R}\|^2}\begin{bmatrix} R_{1_Z} & R_{1_Z}\mathrm{c}_{\beta_2} & R_{1_Z}\mathrm{c}_{\beta_3} \\ 0 & -R_{1_Z}\mathrm{s}_{\beta_2} & -R_{1_Z}\mathrm{s}_{\beta_3} \\ -R_{1_X} & -R_{1_X} & -R_{1_X} \end{bmatrix}\begin{bmatrix} \omega_1 \\ \omega_2 \\ \omega_3 \end{bmatrix}. \tag{8}$$

4 Slip

Because of the kinematic geometry of the sphere driven by three omni-wheels, there will typically be some slip at the contact points between the sphere and omni-wheels. Slip occurs when two contacting surfaces move such that the linear velocity at the contact point is different for each surface. Slip can be quantified in two ways: slip velocity; and slip percentage (or slip ratio). Analyzing the slip factors of the Atlas spherical platform is necessary because almost all cases of angular displacement will cause varying velocities between mating surfaces at their contact points.

To characterize the slip factors of the Atlas platform the linear tangential velocities are used. The slip factors are expressed relative to the Atlas sphere. There are two slip velocity components to be determined: the transverse velocity, $\mathbf{S}_{\perp_k}$, and the tangential velocity, $\mathbf{S}_{\tan_k}$. These two velocity vectors fall on the tangent plane at each contact point of the sphere and the omni-wheel, see Figure 5, and are mutually perpendicular.

The transverse velocity component, $\mathbf{S}_{\perp_k}$, is perpendicular to the free-spinning castor wheel axis. Whereas, the tangential velocity component, $\mathbf{S}_{\tan_k}$, is perpendicular to the omni-wheel driving axis, parallel to the tangential velocity vector, $\mathbf{V}_k$. Both $\mathbf{S}_{\perp_k}$ and $\mathbf{S}_{\tan_k}$ lie in the omni-wheel-sphere tangent plane. The tangential velocity of slip, $\mathbf{S}_{\tan_k}$ lies along the j-axis of the omni-wheel slip frame, illustrated in Figure 5. The transverse velocity component of slip, $\mathbf{S}_{\perp_k}$, lies along the tangential plane of the contact point and the Atlas sphere, which is θ° relative to the k-axis. The tangent plane, which is perpendicular to both the contact point and $\mathbf{R}_k$, can be determined using the angle θ from Equation (2). This indicates that the tangential plane varies with the radius of the Atlas sphere and location of the contact points relative to the XY-plane.

The velocities in the tangential and transverse direction must be found for both the omni-wheels and the Atlas sphere at the contact points. The omni-wheel's tangential-velocities are expressed in the omni-wheel slip frame by Equation (3), and in the inertial frame by Equations (5)-(7). The transverse-velocity of the omni-wheel is 0; this is because there is no actuation of the wheel in that direction. The transverse-velocity of the Atlas sphere at each contact point is unconstrained by the omni-wheel because the castor wheels on the periphery of each omni-wheel are free spinning. The tangential and transverse slip velocity components of the Atlas sphere must be calculated separately.

To compute the sphere linear velocities at the omni-wheel contact points, $\boldsymbol{\Lambda}_k$, $k \in \{1, 2, 3\}$, we use the cross-product of the angular velocity of the Atlas sphere, $\boldsymbol{\Omega}$, and the three radial vectors $\mathbf{R}_k$:

$$\boldsymbol{\Lambda}_k \;=\; \boldsymbol{\Omega} \times \mathbf{R}_k. \tag{9}$$

The velocities must be transformed to the individual omni-wheel slip frames to establish the slip

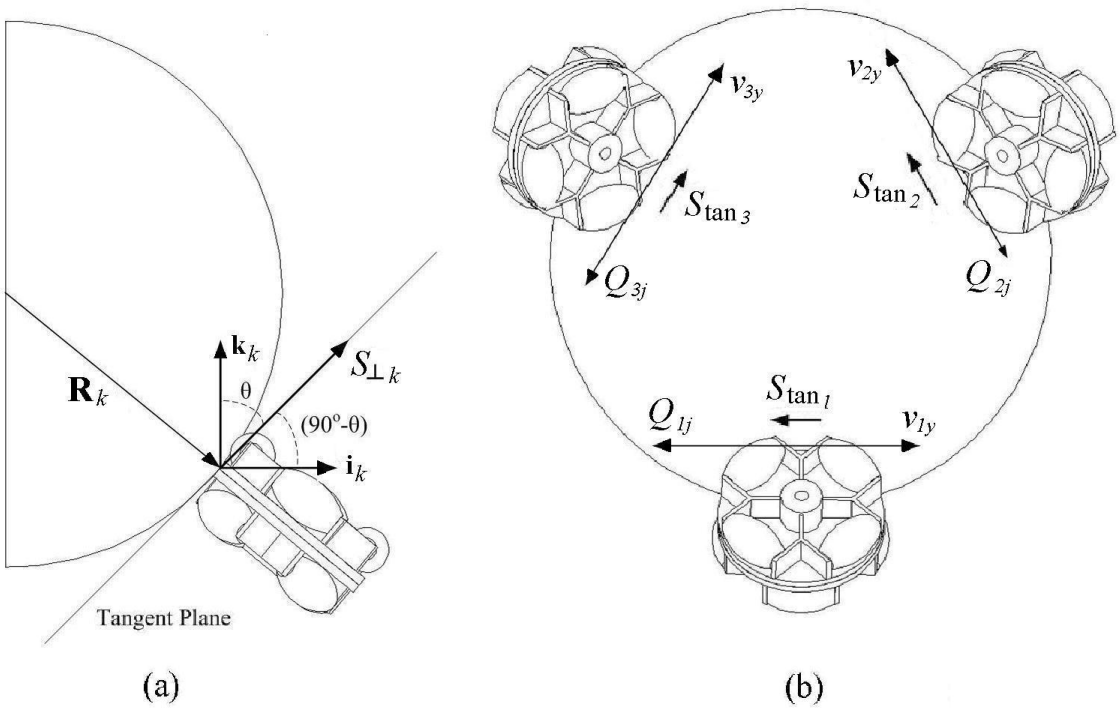

Figure 5: (a) Transverse velocity component and (b) tangential velocity component of slip.

transverse and tangential components:

$$\mathbf{Q}_k \quad = \quad \mathbf{T}_k^{-1}\mathbf{\Lambda}_k, \tag{10}$$

where $\mathbf{Q}_k$ is the linear velocity if the sphere at the k^{th} contact point expressed in the k^{th} omni-wheel slip frame.

4.1 Tangential Slip Velocity Component

First, the tangential slip velocity, $\mathbf{S}_{\tan_k}$, which is in the direction of the j-axis of frame $[i_k, j_k, k_k]$ shall be computed:

$$\mathbf{S}_{\tan_k} \quad = \quad v_{k_y} - Q_{k_j}. \tag{11}$$

Note that both the y-axis and j-axis directions are the same, and hence velocities in these basis directions may be added directly.

4.2 Slip Ratio

The tangential slip velocity $\mathbf{S}_{\tan_k}$ has components due to both the omni-wheel (v_{ky}) and the Atlas sphere (Q_{k_j}). Since these two mating elements posses different velocities at the contact point, there will be a resulting slip ratio. The slip ratio, SR_k, or slip percentage, is a measure of how much

faster $\mathbf{S}_{\tan_k}$ is compared to the Atlas sphere Q_{k_j}:

$$SR_k = \left(\frac{\mathbf{S}_{\tan_k}}{Q_{k_j}} \right) 100. \tag{12}$$

The slip ratio quantifies the slip between the Atlas sphere and the omni-wheel at a specific contact point in the tangential velocity direction. The sign of SR_k determines in what direction on the j-axis (y-axis) the tangential slip velocity is pointing. If the absolute value of SR_k is greater than 100% then the tangential slip velocity is greater than the Atlas sphere's tangential velocity at that contact point. Conversely, if the absolute value of SR_k is below 100% then the Atlas sphere tangential velocity is greater $\mathbf{S}_{\tan_k}$. If both the omni-wheel and the Atlas sphere tangential velocities were identical, then there would be no slip: we would have $\mathbf{S}_{\tan_k} = 0$, and there would be no slip ratio. Alternately, if $Q_{k_j} \approx 0$, then Equation (12) tends towards infinity. Note that achieving tangential slip of zero is a control objective.

4.3 Transverse Slip Velocity

The transverse slip velocity, $\mathbf{S}_{\perp_k}$, relies only on the Atlas sphere's velocity component in the tangent plane perpendicular to the tangential slip velocity, $\mathbf{S}_{\tan_k}$. The omni-wheel does not contribute to the transverse slip velocity because there is no actuation of the omni-wheel in this direction; therefore the slip ratio is always unity since the free-spinning castor wheels will rotate at the same speed as the Atlas sphere in the transverse direction. From Equation (10) for each contact point and the tangential plane geometry:

$$\mathbf{S}_{\perp_k} \;=\; Q_{k_i} \cos\left(90^\circ - \theta\right) + Q_{k_k} \cos\theta. \tag{13}$$

4.4 Slip Velocity Vector

The slip velocity at each contact point, expressed in the plane defined by $\mathbf{S}_{\perp_k}$ and $\mathbf{S}_{\tan_k}$ is simply the vector comprised of the two signed magnitudes:

$$\mathbf{S}_k \;=\; \begin{bmatrix} S_{\perp_k} \\ S_{\tan_k} \end{bmatrix}. \tag{14}$$

5 Examples

The following examples illustrate the levels of slip involved in actuating the Atlas sphere using omni-wheels as discussed above. Clearly, the largest control challenge is coping with the non-holonomic differential constraints arising from the slip induced by the actuation. Regarding trajectory generation there are two ways, conceptually, to deal with the non-integrable velocity constraints and estimate the pose of the sphere at any instant given a set of omni-wheel angular velocity inputs: either numerically integrate the angular velocity relations expressed by Equation (8) based on information embedded in the slip model; or integrate rate sensor output on the sphere to estimate pose. For Atlas sphere orientation control, some form of computed pose state is needed to be compared with the integrated sensed rate output.

k	SR_k (%)	$\mathbf{S}_{\tan_k}$ (m/s)	$\mathbf{S}_{\perp_k}$ (m/s)
1	0	0	0
2	100	0.0850	-0.0274
3	100	0.0850	0.0274

Table 1: Slip for Example 1.

5.1 Example 1

In this example Omni-wheel 1 is given an angular velocity of 1 rad/s, while Omni-wheels 2 and 3 remain stationary. The omni-wheel radius is $r_z = 0.1$ m, while the sphere radial vector components are $R_X = 0.75$ m, $R_Y = 0$ m, $R_Z = -0.25$ m. The computed angular velocity of the sphere is $\Omega_X = -0.04$ rad/s, $\Omega_Y = 0$ rad/s, $\Omega_Z = -0.12$ rad/s, with $\|\mathbf{\Omega}\| = 0.1265$ rad/s. The angular velocity vector of the sphere should generate slip at the contact points with the two fixed omni-wheels.

The output of the slip model is listed in Table 1. As may have been expected, there is no slip on the one rotating omni-wheel, but there is 100% slip on the two stationary wheels.

5.2 Example 2

In this example a pure *roll* rotation (about the X-axis) is generated. The omni-wheel inputs are $\omega_1 = 1$ rad/s, $\omega_2 = -0.5$ rad/s, and $\omega_3 = -0.5$ rad/s. Note: to generate pure *roll* rotation (about the X-axis) we must have $\omega_1 = -\frac{1}{2}\omega_2 = -\frac{1}{2}\omega_3$; to generate pure *pitch* (about the Y-axis) we must have $\omega_1 = 0$, and $\omega_2 = -\omega_3$; to generate pure *yaw* (about the Z-axis) we must have $\omega_1 = \omega_2 = \omega_3$.

k	SR_k (%)	$\mathbf{S}_{\tan_k}$ (m/s)	$\mathbf{S}_{\perp_k}$ (m/s)
1	-566.6667	-0.0850	0
2	566.6667	0.0425	-0.0411
3	566.6667	0.0425	0.0411

Table 2: Slip for Example 2.

For omni-wheel and sphere geometry the same as in Example 1, the outputs are listed in Table 2. It is to be seen that the slip ratio for each omni-wheel is more than 500%. The major conclusion to be drawn from Examples 1 and 2 is that slip is a significant issue for state estimation for pose level kinematics.

6 Conclusions

The Atlas simulator motion platform employs three omni-directional wheels to provide changes in platform orientation. This actuation concept will typically produce slip between the omni-wheels and the Atlas sphere at the contact points. The slip-vectors lie on tangent planes of the

Atlas sphere. The slip is modelled by three parameters: the tangential-slip velocity, $\mathbf{S}_{\tan_k}$; the transverse-slip velocity, $\mathbf{S}_{\perp_k}$; and the slip ratio, SR_k.

Given the non-holonomic velocity constraints of the actuation concept, no integrating factor exists permitting a solution of the associated differential equations. Thus, the orientation of the sphere at any given instant is impossible to determine given a set of omni-wheel angular velocity values. This was the motivation for developing a slip model for the Atlas sphere. This model will be developed and used, together with rate-sensor data, during sphere angular displacements, to control the angular displacement level kinematics of the sphere.

References

[1] M.J.D. Hayes and R.L. Langlois. "Atlas: A Novel Kinematic Architecture for Six DOF Motion Platforms". 2^{nd} *CCToMM Symposium on Machines, Mechanisms and Mechtronics,* Canadian Space Agency, on CD, May 26-27, 2005.

[2] J. Robinson, J.B. Holland, M.J.D. Hayes, and R.L. Langlois. "Velocity Level Control of a Spherical Orienting Device Using Omni-directional Wheels". 2^{nd} *CCToMM Symposium on Machines, Mechanisms and Mechtronics,* Canadian Space Agency, on CD, May 26-27, 2005.

[3] S. Jonsson. "New AGV with Revolutionary Movement". *Proc.* 3^{rd} *Int. Conf. on Automated Guided Vehicles,* Stockholm, pages 135–144, 1985.

[4] J. Angeles. *Fundamentals of Robotic Mechanical Systems: Theory, Methods, and Algorithms.* Springer-Verlag, New York, N.Y., U.S.A., 1997.

[5] F. Williams, E.R. Laithwaite, and G.F. Eastham. "Development and Design of Spherical Induction Motors". *Proc IEEE*, vol. 47:471–484, Dec. 1959.

[6] R.B. Roth and K.-M. Lee. "Design Optimization of a Three-Degree-of-Freedom Variable Reluctance Spherical Wrist Motor". *ASME J. Eng. Industry*, vol. 117:378–388, 1995.

[7] S. Toyama, S. Sugitani, G. Zhang, Y. Miyatani, and K Nakamura. "Multi Degree of Freedom Spherical Ultrasonic Motor". *Proc 1995 IEEE Int. Conf. Robotic and Automation*, pages 2935–2940, 1995.

[8] G.S. Chirikjian and D. Stein. "Kinematic Design and Commutation of a Spherical Stepper Motor". *IEEE/ASME Transactions on Mechatronics*, vol. 4, no. 4:342–353, 1999.

[9] R. Williams, D. Carter, P. Gallina, and G. Rosati. "Dynamics Model with Slip for Wheeled Omni-Directional Robots". *IEEE Transactions on Robotic and Automation*, vol. 18, no. 3:285–293, 2002.